*Acta Cryst.* (1982). B**38**, 1990–2000

# Crystallographic Study of the 1,5-Diazabicyclo[3.3.0]octadienedione (9,10-Dioxabimane) System. Crystal Structures and Molecular Conformations of 2,8-Dimethyl-1,5-diazabicyclo[3.3.0]octa-2,7-diene-4,6-dione [*syn*-($CH_3$,H)-9,10-dioxabimane], 2,6-Dimethyl-1,5-diazabicyclo[3.3.0]octa-2,6-diene-4,8-dione [*anti*-($CH_3$,H)-9,10-dioxabimane] and 2,6-Dimethyl-3,5-dioxo-4,11-diazatricyclo[5.3.1.$0^{4,11}$]undeca-1,6-diene-9,9-dicarbonitrile {$\mu$-[$C(CN)_2$]-*syn*-($CH_2$,$CH_3$)-9,10-dioxabimane}

BY ISRAEL GOLDBERG

*Department of Chemistry, Tel-Aviv University,* 69978 *Ramat Aviv, Israel*

JOEL BERNSTEIN

*Department of Chemistry, Ben-Gurion University,* 84120 *Beer-Sheva, Israel*

AND EDWARD M. KOSOWER

*Departments of Chemistry, Tel-Aviv University,* 69978 *Ramat Aviv, Israel and State University of New York, Stony Brook, NY* 11794, *USA*

(*Received* 23 *July* 1981; *accepted* 20 *January* 1982)

## Abstract

The structures of three representative 1,5-diazabicyclo-[3.3.0]octadienedione (9,10-dioxabimane) compounds have been determined. *syn*-($CH_3$,H)-9,10-dioxabimane, $C_8H_8N_2O_2$, $M_r$ = 164·17, crystallizes in space group *Pnma* with $a$ = 13·987 (3), $b$ = 6·651 (1), $c$ = 8·398 (2) Å and $Z$ = 4; conventional and deformation refinements led to $R$ = 0·046, 0·047 for 960, 1334 reflections, respectively. *anti*-($CH_3$,H)-9,10-dioxabimane, $C_8H_8N_2O_2$, $M_r$ = 164·17, crystallizes in $P\bar{1}$ with $a$ = 6·374 (1), $b$ = 7·595 (1), $c$ = 8·442 (3) Å, $\alpha$ = 101·24 (2), $\beta$ = 95·51 (3), $\gamma$ = 92·44 (1)° and $Z$ = 2; $R$ = 0·053 for 1426 reflections. $\mu$-[$C(CN)_2$]-*syn*-($CH_2$,$CH_3$)-9,10-dioxabimane, $C_{13}H_{10}N_4O_2$, $M_r$ = 254·25, crystallizes in space group $P2_1/c$ with $a$ = 9·975 (4), $b$ = 7·413 (2), $c$ = 17·008 (5) Å, $\beta$ = 100·10 (3)° and $Z$ = 4; $R$ = 0·047 for 1355 reflections. The simplest unbridged *syn* and *anti* bicyclic derivatives are planar, partially conjugated and flexible (mainly about the central N–N bond) systems. The corresponding crystals consist of similarly layered structures. The tricyclic bridged 9,10-dioxabimane is strained and less conjugated, exhibiting a bent but more rigid conformation. The observed packing arrangements reveal a significant contribution of specific C–H···O interactions to the crystal structure of several dioxabimanes.

## Introduction

The attractive simplicity of the 1,5-diazabicyclo-[3.3.0]octadienediones (9,10-dioxabimanes) as well as their importance in chemical (Kosower & Pazhenchevsky, 1980; Kosower, Pazhenchevsky, Dodiuk, Kanety & Faust, 1981), photophysical (Huppert, Dodiuk, Kanety & Kosower, 1979), photochemical and biological (Kosower, Newton, Kosower & Ranney, 1980; Kosower, Kosower, Zipser, Faltin & Shomrat, 1981) investigations made a careful study of their basic structural parameters essential for further work. We report in the present article a study of three representative 9,10-dioxabimanes or 'bimanes', each being the simplest derivatives of their class thus far available in the form of crystals suitable for detailed structural investigations. The three compounds are: *syn*-($CH_3$,H)-bimane [*syn*-($CH_3$,H)B; (I)], *anti*-($CH_3$,H)-bimane [*anti*-($CH_3$,H)B; (II)] and $\mu$-(dicyanomethylene)-*syn*-($CH_2$,$CH_3$)-bimane {$\mu$-[$C(CN)_2$]-*syn*-($CH_2$,$CH_3$)B; (III)}. The nomenclature for the bimanes has been set forth in a previous publi-

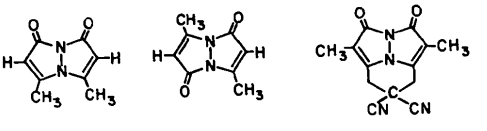

(I) (II) (III)

0567-7408/82/071990-11$01.00 

cation (Kosower & Pazhenchevsky, 1980). Preliminary accounts of other bimane crystal structures have been given elsewhere (Bernstein, Goldstein & Goldberg, 1980; Goldberg, 1980).

## Experimental

The experimental data detailed below were obtained separately in three different laboratories under non-identical conditions and the accuracy of the achieved results varies, therefore, from structure to structure.

*syn*-($CH_3$,H)B (I)

A well formed parallelepiped crystal of approximate dimensions 0·25 × 0·25 × 0·40 mm was selected for the analysis. X-ray diffraction showed orthorhombic symmetry and the systematic absences ($0kl$ with $k + l$ odd, $hk0$ with $h$ odd) expected for space group *Pnma*. Diffraction data were measured on a Syntex $P\bar{1}$ autodiffractometer equipped with a graphite monochromator, employing Mo $K\alpha$ radiation ($\lambda_{mean}$ = 0·71069 Å). Since there is an apparent phase transition in the crystal structure at about 183 K, all measurements were carried out at 193 ± 3 K; our efforts to produce a single crystal of the low-temperature phase by slow cooling below the transition point failed. Crystal data are given in the *Abstract* and Table 1.

Accurate cell constants were determined by least squares from the setting angles of 15 reflections with $2\theta$ between 14·5 and 25·8° centered on the diffractometer. Intensity data of 1820 unique observations were collected in the $\omega$–$2\theta$ scan mode out to $2\theta = 70°$ (sin $\theta/\lambda$ = 0·807 Å$^{-1}$). Reflections were scanned at a constant rate of 3° min$^{-1}$ from 1·1° below $K\alpha_1$ to 1·1° above $K\alpha_2$ with stationary background measurements at the beginning and end of each scan. The intensities of three standard reflections, recorded every 97 reflections varied by less than 2% about their mean during the course of data collection. The data were corrected for Lorentz and polarization effects, but not for absorption or secondary extinction.

Table 1. *Additional crystal data*

(*a*) *syn*-($CH_3$,H)B (I)

*Pnma*, $F(000)$ = 344, $\mu$(Mo $K\alpha$) = 0·11 mm

| At 298 K | At 193 K |
|---|---|
| $a$ = 13·987 (3) Å | $a$ = 13·970 (2) Å |
| $b$ = 6·651 (1) | $b$ = 6·547 (1) |
| $c$ = 8·398 (2) | $c$ = 8·372 (1) |
| $V$ = 781·2 Å$^3$ | $V$ = 765·7 Å$^3$ |
| $D_c$ = 1·395 Mg m$^{-3}$ | $D_c$ = 1·424 Mg m$^{-3}$ |

(*b*) *anti*-($CH_3$,H)B (II)

$V$ = 398·2 Å$^3$
$F(000)$ = 172
$D_c$ = 1·369 Mg m$^{-3}$
$\mu$(Mo $K\alpha$) = 0·11 mm$^{-1}$

(*c*) $\mu$-[C(CN)$_2$]-*syn*-($CH_2$,$CH_3$)B (III)

$V$ = 1238·2 Å$^3$
$F(000)$ = 528
$D_c$ = 1·364 Mg m$^{-3}$
$\mu$(Mo $K\alpha$) = 0·11 mm$^{-1}$

A successful solution of the phase problem was obtained by the systematic Patterson search method of Braun, Hornstra & Leenhouts (1969). The structure was found to be layered with all nonhydrogen atoms located on the crystallographic mirror planes at $y = \frac{1}{4}$ and $y = \frac{3}{4}$, a circumstance which could explain why our initial attempts to solve the phase problem by a routine application of direct methods had failed. Subsequent conventional refinement was based on 960 observations above threshold, $F_o^2 \geq 3\sigma(F_o^2)$, excluding four extremely strong reflections (200, 101, 020, 040) which were inaccurately measured and probably affected also by extinction. The heavy-atom model was refined to $R$ = 0·084. At this stage all the H atoms were clearly located on a difference map, with peak heights ranging from 0·40 to 0·65 e Å$^{-3}$. Four of these (the two H atoms attached to C at positions 3 and 7 as well as one H of each methyl group) were found to be situated in special positions on the mirror plane, in agreement with the assumed symmetry.

Full-matrix least-squares anisotropic refinement of the nonhydrogen and isotropic refinement of the H atoms gave a final $R$ = 0·046 ($R$ = 0·066 for all 1600 non-zero reflections).* Parameters of the H atoms were adjusted with low-order data only, sin $\theta/\lambda \leq 0{\cdot}55$ Å$^{-1}$. Altogether there were 93 parameters in the refinement. At convergence the final goodness of fit was 1·23. The quantity minimized was $\sum w(\Delta F)^2$, where $w = 1/\sigma^2(F_o)$; the resulting distribution of $\langle w(\Delta F)^2 \rangle$ as a function of sin $\theta/\lambda$ was reasonably constant, except for a small number of very-low-order reflections. No significant changes were observed in the positional parameters of the atomic nuclei of C, N and O when the least-squares computation was based on either of the following weighting schemes: (*a*) $w(F_o) = 1{\cdot}0$, and (*b*) $w(F_o) = \exp(7 \sin^2 \theta/\lambda^2)/\sigma^2(F_o)$ (Dunitz & Seiler, 1973). In this, as well as in the subsequent refinements referred to below, the spherical free-atom form factors for C, N and O were taken from *International Tables for X-ray Crystallography* (1974), those for H from Stewart, Davidson & Simpson (1965). In the final Fourier map of residual density the highest peaks (≤0·2 e Å$^{-3}$) were centered on the various bonds of the molecule (Fig. 1*a*).

In view of the high symmetry of the molecular structure and the relatively good quality of the diffraction data, the calculation of an experimental map of electron density distribution about the molecular framework seemed worthwhile. For this aim, the structural parameters were subjected to further least-

* Lists of structure factors and anisotropic thermal parameters for compounds (I) (conventional and deformation refinements), (II) and (III) have been deposited with the British Library Lending Division as Supplementary Publication No. SUP 36765 (19 pp.). Copies may be obtained through The Executive Secretary, International Union of Crystallography, 5 Abbey Square, Chester CH1 2HU, England.

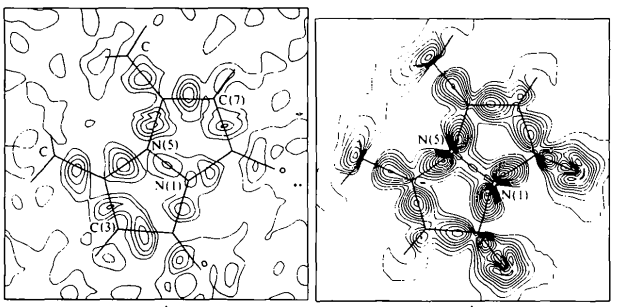


Fig. 1. Two sections of electron density Fourier syntheses through the molecular plane: (*a*) conventional difference map, (*b*) static density map after the deformation refinement. Contour lines are drawn at intervals of 0·05 e Å$^{-3}$, negative contour lines being omitted for clarity. Standard error is estimated to be approximately 0·05 e Å$^{-3}$.

Table 2. *Positional and isotropic thermal parameters of syn-*$(CH_3,H)B$

For non-H atoms $U_{eq} = \frac{1}{3}(U^{11} + U^{22} + U^{33})$, where $U^{ii}$ are diagonal elements of the anisotropic tensor transformed to a Cartesian system.

| | *x* | *y* | *z* | $U_{eq}/U$ (Å$^2$) |
|---|---|---|---|---|
| (*a*) Conventional refinement | | | | |
| N(1) | −0·0008 (1) | 0·25 | 0·0862 (2) | 0·033 |
| C(2) | −0·0852 (1) | 0·25 | −0·0068 (3) | 0·032 |
| C(3) | −0·0492 (2) | 0·25 | −0·1685 (3) | 0·036 |
| C(4) | 0·0480 (2) | 0·25 | −0·1689 (3) | 0·031 |
| N(5) | 0·0781 (1) | 0·25 | −0·0129 (2) | 0·032 |
| C(6) | 0·1600 (1) | 0·25 | 0·0804 (3) | 0·028 |
| C(7) | 0·1332 (1) | 0·25 | 0·2353 (3) | 0·033 |
| C(8) | 0·0293 (2) | 0·25 | 0·2473 (3) | 0·032 |
| O(9) | −0·1659 (1) | 0·25 | 0·0491 (2) | 0·045 |
| O(10) | −0·0250 (1) | 0·25 | 0·3605 (2) | 0·047 |
| C(11) | 0·1168 (2) | 0·25 | −0·3042 (3) | 0·048 |
| C(12) | 0·2568 (1) | 0·25 | 0·0075 (3) | 0·037 |
| H(3) | −0·090 (2) | 0·25 | −0·263 (4) | 0·057 (8) |
| H(7) | 0·178 (2) | 0·25 | 0·318 (3) | 0·038 (7) |
| H(11*A*) | 0·079 (2) | 0·25 | −0·399 (4) | 0·060 (8) |
| H(11*B*) | 0·159 (1) | 0·127 (3) | −0·299 (2) | 0·069 (6) |
| H(12*A*) | 0·303 (2) | 0·25 | 0·092 (4) | 0·048 (7) |
| H(12*B*) | 0·264 (1) | 0·128 (3) | −0·056 (2) | 0·047 (5) |
| (*b*) Deformation refinement | | | | |
| N(1) | −0·0008 (3) | 0·25 | 0·0858 (3) | 0·031 |
| C(2) | −0·0848 (2) | 0·25 | −0·0061 (4) | 0·029 |
| C(3) | −0·0496 (2) | 0·25 | −0·1688 (3) | 0·034 |
| C(4) | 0·0483 (3) | 0·25 | −0·1685 (4) | 0·028 |
| N(5) | 0·0781 (3) | 0·25 | −0·0130 (3) | 0·030 |
| C(6) | 0·1598 (2) | 0·25 | 0·0797 (4) | 0·026 |
| C(7) | 0·1334 (2) | 0·25 | 0·2360 (3) | 0·031 |
| C(8) | 0·0292 (2) | 0·25 | 0·2470 (4) | 0·030 |
| O(9) | −0·1660 (4) | 0·25 | 0·0495 (3) | 0·043 |
| O(10) | −0·0251 (3) | 0·25 | 0·3607 (6) | 0·045 |
| C(11) | 0·1163 (2) | 0·25 | −0·3038 (3) | 0·045 |
| C(12) | 0·2563 (2) | 0·25 | 0·0082 (2) | 0·035 |
| H(3) | −0·089 (2) | 0·25 | −0·260 (4) | 0·057 |
| H(7) | 0·176 (2) | 0·25 | 0·318 (3) | 0·038 |
| H(11*A*) | 0·077 (2) | 0·25 | −0·397 (4) | 0·060 |
| H(11*B*) | 0·158 (2) | 0·128 (4) | −0·298 (2) | 0·069 |
| H(12*A*) | 0·302 (2) | 0·25 | 0·094 (3) | 0·048 |
| H(12*B*) | 0·264 (1) | 0·129 (4) | −0·055 (2) | 0·047 |

squares refinement with deformation functions according to the model of Hirshfeld (1977), using 1334 available data with $|F_o|^2 \geq \sigma(F_o^2)$. The deformation density, which adds to the static free-atom density, was expanded in a basis of atomic multipole functions, assuming exact *mm* symmetry for the molecular structure. All the H atoms were constrained to have identical deformation coefficients, assuming cylindrical symmetry about their bonding direction.

In this refinement, 87 standard (fractional coordinates of all atoms, anisotropic temperature factors of nonhydrogen atoms and a scale factor) and 115 deformation parameters were adjusted against 1334 observations; the atomic form factor of H was contracted to an effective nuclear charge of 1·2. Due to the absence of reliable data on internal vibrations in the C—H bonds, the previously determined H-atom thermal parameters were not refined further. Refinement converged smoothly to $R = 0{\cdot}047$, $R'_w = [\sum w(F_o^2 - F_c^2)^2/\sum wF_o^4]^{1/2} = 0{\cdot}076$ with $w = 1/\sigma^2(F_o^2)$, and the goodness-of-fit was 0·98. The final fractional atomic coordinates resulting from both types of refinement are compared in Table 2. The static deformation density map is illustrated in Fig. 1(*b*). Some differences between the final atomic positions obtained from the conventional and deformation refinements can be observed. They are reflected mainly in a significant increase (*ca* $3\sigma$) of the C(3)—C(4) and C(6)—C(7) lengths and a considerable decrease of the peripheral C—$CH_3$ lengths (Table 5). As expected, the thermal parameters obtained from a refinement with free-atom form factors (particularly $U^{11}$ and $U^{33}$) are systematically about 10–20% larger than those based on the deformation model which takes into account the asperical electron density distribution.

*anti-*$(CH_3,H)B$ (II)

Colorless triclinic crystals of the compound were obtained by slow evaporation from an acetonitrile solution. A platelet measuring approximately 0·1 × 0·2 × 0·4 mm was selected for the analysis and mounted on a Nonius CAD-4 diffractometer. Accurate cell constants (*Abstract*) were obtained by a least-squares procedure applied to 18 reflections with $14 < \theta < 18°$ at the beginning of data collection.

Three-dimensional X-ray diffraction data were collected to $\theta = 30°$ at room temperature by the use of graphite-monochromatized Mo $K\alpha$ radiation ($\lambda_{mean}$ = 0·71069 Å), and an $\omega$–$2\theta$ scan technique with scan width of $(1{\cdot}0 + 0{\cdot}35 \tan\theta)°$. The scan rate varied between 2·5 and 5·0° min$^{-1}$, according to the detected intensity. All data in one half of the available reciprocal space ($\pm h$, $\pm k$, $l$) were measured. Three intensity-control reflections, monitored after each hour, showed no decay of the crystal. The intensities were corrected for Lorentz and polarization effects and variable

Table 3. *Positional and isotropic thermal parameters of anti-*$(CH_3,H)B$

For non-H atoms $U_{eq} = \frac{1}{3}(U^{11} + U^{22} + U^{33})$, where $U^{ii}$ are diagonal elements of the anisotropic tensor transformed to a Cartesian system.

| | $x$ | $y$ | $z$ | $U_{eq}/U$ (Å$^2$) |
|---|---|---|---|---|
| N(1) | 0·9121 (3) | 0·9616 (2) | 0·5233 (2) | 0·051 |
| C(2) | 0·8941 (3) | 0·7807 (3) | 0·4529 (3) | 0·043 |
| C(3) | 1·0563 (4) | 0·7457 (3) | 0·3647 (3) | 0·050 |
| C(4) | 1·1864 (3) | 0·9085 (3) | 0·3726 (3) | 0·048 |
| C(5) | 0·7152 (4) | 0·6647 (3) | 0·4801 (3) | 0·062 |
| O(6) | 1·3432 (3) | 0·9406 (3) | 0·3103 (2) | 0·074 |
| N(7) | 0·9663 (3) | 0·9108 (2) | −0·0232 (3) | 0·057 |
| C(8) | 0·7843 (3) | 0·8826 (3) | 0·0457 (3) | 0·042 |
| C(9) | 0·7398 (3) | 1·0396 (3) | 0·1356 (3) | 0·046 |
| C(10) | 0·8955 (3) | 1·1795 (3) | 0·1245 (3) | 0·045 |
| C(11) | 0·6736 (4) | 0·7018 (3) | 0·0136 (3) | 0·057 |
| O(12) | 0·9168 (3) | 1·3395 (2) | 0·1826 (2) | 0·064 |
| H(3) | 1·075 (3) | 0·637 (3) | 0·291 (3) | 0·045 |
| H(5*A*) | 0·700 (4) | 0·662 (3) | 0·593 (3) | 0·060 |
| H(5*B*) | 0·726 (4) | 0·544 (4) | 0·420 (3) | 0·060 |
| H(5*C*) | 0·577 (4) | 0·704 (3) | 0·427 (3) | 0·060 |
| H(9) | 0·624 (4) | 1·063 (3) | 0·192 (3) | 0·045 |
| H(11*A*) | 0·556 (4) | 0·703 (3) | 0·076 (3) | 0·060 |
| H(11*B*) | 0·771 (4) | 0·613 (3) | 0·043 (3) | 0·060 |
| H(11*C*) | 0·621 (4) | 0·665 (3) | −0·098 (4) | 0·060 |

measuring time, but not for absorption or extinction. A total of 2193 reflections were collected, of which 2067 were unique; the 126 reflections that were each measured twice were averaged, giving a merging residual of $R = 0{\cdot}021$. 1430 observations satisfied the condition $F_o^2 \geq 3\sigma(F_o^2)$ and were used in the final refinement.

The structure was solved by weighted-tangent-formula refinement (*MULTAN* 74; Main, Woolfson, Lessinger, Germain & Declercq, 1974) applied to 160 reflections with $|E| \geq 1{\cdot}75$; the space group $P\bar{1}$ was assumed on the basis of relevant statistical distributions of the intensity data set, and eventually confirmed by successful refinement. The asymmetric unit is composed of the halves of two independent molecules, each of which is located on a crystallographic center of symmetry at 0,0,0 and 0,0,$\frac{1}{2}$ respectively.

Refinement was carried out by full-matrix least squares including the positional and anisotropic thermal parameters for the non-hydrogen atoms. The eight H atoms were located in a difference synthesis. Positional parameters of the H atoms were adjusted with low-order data below $\sin\theta/\lambda = 0{\cdot}55$ Å$^{-1}$, but no attempt was made to refine the isotropic temperature factors which were set to $U = 0{\cdot}045$ and $0{\cdot}060$ Å$^2$ for the =C−H and $-CH_3$ groups respectively. Refinement was terminated with $R = 0{\cdot}053$ for 1426 observations;* four strong low-angle reflections were omitted in the last cycle of refinement. The quantity minimized was $\sum w(\Delta F)^2$, where $w = 1{\cdot}0$. Use of a weighting scheme in which equal weights are assigned to all observations in the refinement process was suggested by a reasonably constant distribution of $\langle w(\Delta F)^2 \rangle$ with increasing $\sin\theta/\lambda$. Refinement based on the experimental weights $[1/\sigma^2(F_o)]$ gave a relatively high value for the weighted $R$ $\{[\sum w(\Delta F)^2/\sum wF_o^2]^{1/2} = 0{\cdot}063\}$. There were no significant features in the difference map after the refinement was complete; the highest peak and deepest trough were 0·22 and −0·20 e Å$^{-3}$ respectively. The final atomic parameters are given in Table 3.

* See deposition footnote.

### $\mu$-$[C(CN)_2]$-*syn*-$(CH_2,CH_3)B$ (III)

Approximate cell dimensions were determined from preliminary Weissenberg and precession photographs. The diffraction pattern shows Laue symmetry $2/m$ and systematic absences $0k0$ with $k$ and $h0l$ with $l$ odd uniquely determining the space group $P2_1/c$. Accurate lattice parameters (*Abstract*) and an orientation matrix were obtained by a least-squares fit to the setting angles ($11 < \theta < 18°$) of 15 reflections, centered on a Syntex $P2_1$ four-circle diffractometer.

Intensities were measured with graphite-monochromatized Mo $K\alpha$ radiation ($\lambda_{mean} = 0{\cdot}71069$ Å) for $2\theta$ between 1 and 55°. The scan rate for all reflections was 2° min$^{-1}$ over the peak width with a $2\theta$ range

Table 4. *Positional and isotropic thermal parameters of* $\mu$-$[C(CN)_2]$-*syn*-$(CH_2,CH_3)B$

For non-H atoms $U_{eq} = \frac{1}{3}(U^{11} + U^{22} + U^{33})$, where $U^{ii}$ are diagonal elements of the anisotropic tensor transformed to a Cartesian system.

| | $x$ | $y$ | $z$ | $U_{eq}/U$ (Å$^2$) |
|---|---|---|---|---|
| N(1) | 0·5863 (2) | 0·4392 (3) | 0·1283 (1) | 0·040 |
| C(2) | 0·6228 (3) | 0·3367 (4) | 0·0639 (2) | 0·043 |
| C(3) | 0·6921 (3) | 0·4628 (4) | 0·0179 (2) | 0·041 |
| C(4) | 0·6980 (3) | 0·6233 (4) | 0·0549 (2) | 0·037 |
| N(5) | 0·6258 (2) | 0·6172 (3) | 0·1189 (1) | 0·036 |
| C(6) | 0·6817 (3) | 0·6862 (4) | 0·1945 (2) | 0·035 |
| C(7) | 0·6706 (3) | 0·5651 (4) | 0·2513 (2) | 0·038 |
| C(8) | 0·6148 (3) | 0·3981 (4) | 0·2122 (2) | 0·040 |
| O(9) | 0·5981 (2) | 0·1766 (3) | 0·0543 (1) | 0·057 |
| O(10) | 0·5961 (2) | 0·2522 (3) | 0·2400 (1) | 0·057 |
| C(11) | 0·7477 (4) | 0·4080 (5) | −0·0536 (2) | 0·062 |
| C(12) | 0·7040 (3) | 0·5833 (5) | 0·3397 (2) | 0·054 |
| C(13) | 0·7645 (3) | 0·8004 (4) | 0·0456 (2) | 0·042 |
| C(14) | 0·7417 (3) | 0·8697 (4) | 0·1915 (2) | 0·043 |
| C(15) | 0·8403 (3) | 0·8659 (4) | 0·1294 (2) | 0·041 |
| C(16) | 0·9543 (3) | 0·7422 (5) | 0·1591 (2) | 0·047 |
| C(17) | 0·8994 (3) | 1·0471 (5) | 0·1192 (2) | 0·054 |
| N(18) | 1·0385 (3) | 0·6434 (5) | 0·1832 (2) | 0·073 |
| N(19) | 0·9463 (3) | 1·1816 (4) | 0·1078 (2) | 0·083 |
| H(11*A*) | 0·690 | 0·406 | −0·101 | 0·060 |
| H(11*B*) | 0·804 | 0·302 | −0·043 | 0·060 |
| H(11*C*) | 0·826 | 0·489 | −0·068 | 0·060 |
| H(12*A*) | 0·631 | 0·583 | 0·365 | 0·060 |
| H(12*B*) | 0·759 | 0·480 | 0·366 | 0·060 |
| H(12*C*) | 0·768 | 0·681 | 0·357 | 0·060 |
| H(13*A*) | 0·694 | 0·887 | 0·027 | 0·045 |
| H(13*B*) | 0·833 | 0·788 | 0·007 | 0·045 |
| H(14*A*) | 0·790 | 0·904 | 0·242 | 0·045 |
| H(14*B*) | 0·662 | 0·950 | 0·176 | 0·045 |

below $K\alpha_1$ and above $K\alpha_2$ of 1·2°. No crystal decomposition was detectable during the measurements. The data were processed in the usual manner including corrections for background and the Lp factor, but not for absorption or extinction; the reduced data set contained 2846 independent observations.

The structure was solved by a straightforward application of *MULTAN* 74. Refinement was carried out by full-matrix least squares, first isotropically ($R$ = 10%), then anisotropically ($R$ = 7·5%). All H atoms could be located by a Fourier difference synthesis very near to their expected positions, the heights of the corresponding peaks ranging from 0·35 to 0·50 e Å$^{-3}$. They were included in the structural model with isotropic temperature factors set to $U$ = 0·045 Å$^2$ for the methylene groups and $U$ = 0·060 Å$^2$ for the peripheral methyl substituents. The refinement converged to $R$ = 0·047 and $R_w = [\sum w(\Delta F)^2/\sum wF_o^2]^{1/2}$ = 0·052.* The weights $w = 1/\sigma^2(F_o)$ were slightly reduced for the strongest reflections to account for an additional uncertainty due to possible extinction. The final value of $[\sum w(\Delta F)^2/(n-m)]^{1/2}$ is 1·61 for $n$ = 1355 observations above the threshold $[|F_o|^2 \geq 3\sigma(F_o^2)]$ and $m$ = 172 refined parameters. A final difference map showed no peaks whose absolute heights exceeded 0·23 e Å$^{-3}$. Atomic parameters at convergence of the refinement are listed in Table 4.

## Discussion of results

*The molecular structures*

The molecular configurations of *syn*-($CH_3$,H)B, *anti*-($CH_3$,H)B and $\mu$-[$C(CN)_2$]-*syn*-($CH_2$,$CH_3$)B are illustrated in Figs. 2, 3 and 4 respectively, together with the crystallographic atom numbering used in this report. The covalent distances and angles which were not corrected for the effects of thermal motion (see below) are presented in Tables 5, 6 and 7. Most of the chemically equivalent bond distances in each molecule are essentially equal, the spread about their mean values being within 1·5$\sigma$. In (I) there are some statistically significant discrepancies between equivalent bonds, the trend being similar for the two refinements. Some of the discrepancies may be due in part to different overlap interactions imposed on the two rings of (I) in the crystal (see below).

* See deposition footnote.

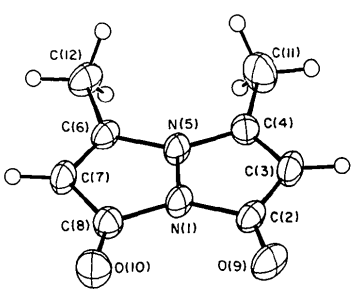


Fig. 2. A perspective drawing of the molecular structure of *syn*-($CH_3$,H)B showing the numbering. Thermal ellipsoids correspond to 50% probability.

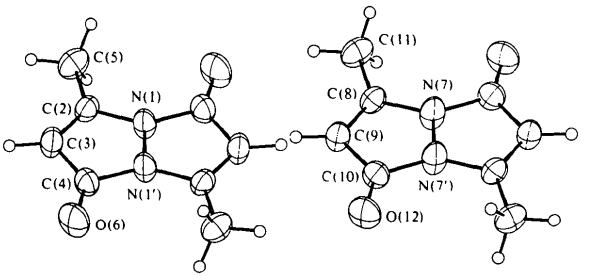


Fig. 3. Molecular structure of *anti*-($CH_3$,H)B; the full molecules derived from the two independent half-molecules of the asymmetric unit are shown.

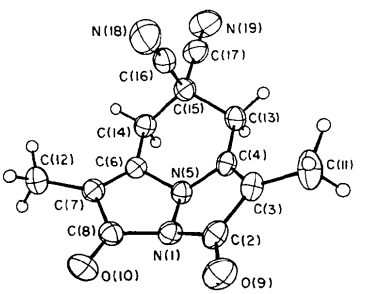


Fig. 4. Molecular structure of $\mu$-[$C(CN)_2$]-*syn*-($CH_2$,$CH_3$)B. Thermal ellipsoids correspond to 40% probability.

The molecular frameworks of (I) and (II), excluding the H atoms, are planar. In the crystal structure of (I) all nonhydrogen and four of the H atoms are located on the crystallographic mirror planes; for structure (II), in which the molecules occupy sites of crystallographic inversion, the deviations from planarity are within 0·01 Å. The two central N atoms in both compounds are thus best described as $sp^2$-hybridized. On the other hand, the bimane framework of compound (III) is significantly bent about the N–N bond, the dihedral angle between least-squares planes of the two five-membered rings being 139·3°. Furthermore, atoms C(4) and C(6) deviate about 0·06 and 0·08 Å from the respective mean planes of the individual rings toward the bridging group. The sum of angles around N(5) (338°) becomes, therefore, smaller than that around N(1) (343°).

Changes in the pyramidal nature of the N lead to marked changes in the detailed geometry of the molecules. For example, the N–N bonds in (I) (1·378 Å) and (II) (av. 1·370 Å) show considerable shortening; in the bent molecule (III) this bond is longer by more than 3$\sigma$ (1·394 Å). The differences are even more pronounced in the adjacent C–N bonds, the N–C(=C) distances varying from 1·376–1·377 Å in

Table 5. *Bond distances* (Å) *and bond angles* (°) *in* *syn*-$(CH_3,H)B$

Columns (*a*) and (*b*) refer to conventional and deformation refinements. Bond distances are not corrected for thermal motion.

| | (*a*) | (*b*) |
|---|---|---|
| N(1)–C(2) | 1·414 (3) | 1·404 (5) |
| N(1)–N(5) | 1·379 (2) | 1·378 (5) |
| N(1)–C(8) | 1·412 (3) | 1·413 (4) |
| C(2)–C(3) | 1·445 (4) | 1·449 (4) |
| C(2)–O(9) | 1·220 (3) | 1·225 (6) |
| C(3)–C(4) | 1·358 (3) | 1·367 (4) |
| C(4)–N(5) | 1·372 (3) | 1·367 (4) |
| C(4)–C(11) | 1·485 (4) | 1·478 (4) |
| N(5)–C(6) | 1·385 (3) | 1·381 (5) |
| C(6)–C(7) | 1·350 (3) | 1·359 (4) |
| C(6)–C(12) | 1·484 (3) | 1·474 (4) |
| C(7)–C(8) | 1·456 (3) | 1·460 (4) |
| C(8)–O(10) | 1·214 (3) | 1·216 (6) |
| C(3)–H(3) | 0·97 (3) | 0·94 (3) |
| C(7)–H(7) | 0·93 (3) | 0·91 (3) |
| C(11)–H(11*A*) | 0·95 (3) | 0·95 (3) |
| C(11)–H(11*B*) | 1·00 (2) | 0·99 (2) |
| C(12)–H(12*A*) | 0·96 (3) | 0·96 (3) |
| C(12)–H(12*B*) | 0·96 (2) | 0·96 (2) |
| N(5)–N(1)–C(2) | 109·6 (2) | 109·8 (3) |
| C(8)–N(1)–C(2) | 140·7 (2) | 140·5 (3) |
| C(8)–N(1)–N(5) | 109·7 (2) | 109·7 (3) |
| N(1)–C(2)–C(3) | 103·0 (2) | 103·4 (3) |
| N(1)–C(2)–O(9) | 124·0 (2) | 124·4 (3) |
| O(9)–C(2)–C(3) | 132·9 (2) | 132·2 (3) |
| C(2)–C(3)–C(4) | 110·5 (2) | 109·8 (3) |
| C(3)–C(4)–N(5) | 107·7 (2) | 107·8 (3) |
| C(3)–C(4)–C(11) | 130·5 (2) | 129·9 (3) |
| N(5)–C(4)–C(11) | 121·8 (2) | 122·3 (3) |
| N(1)–N(5)–C(6) | 108·7 (2) | 108·9 (3) |
| C(4)–N(5)–N(1) | 109·2 (2) | 109·2 (3) |
| C(4)–N(5)–C(6) | 142·1 (2) | 141·9 (3) |
| N(5)–C(6)–C(7) | 108·2 (2) | 108·4 (3) |
| N(5)–C(6)–C(12) | 121·4 (2) | 121·8 (3) |
| C(7)–C(6)–C(12) | 130·3 (2) | 129·7 (3) |
| C(6)–C(7)–C(8) | 110·0 (2) | 109·4 (3) |
| N(1)–C(8)–O(10) | 124·0 (2) | 124·2 (4) |
| C(7)–C(8)–N(1) | 103·3 (2) | 103·6 (3) |
| C(7)–C(8)–O(10) | 132·6 (2) | 132·2 (4) |

Table 6. *Bond distances* (Å) *and bond angles* (°) *in* *anti*-$(CH_3,H)B$

Atoms marked by an asterisk are related to the corresponding unmarked atoms by inversion at 1,1,0 or 1,1,$\frac{1}{2}$.

| | | | |
|---|---|---|---|
| N(1)–N(1*) | 1·368 (4) | N(7)–N(7*) | 1·372 (4) |
| N(1)–C(2) | 1·380 (3) | N(7)–C(8) | 1·374 (3) |
| C(2)–C(3) | 1·337 (3) | C(8)–C(9) | 1·338 (3) |
| C(2)–C(5) | 1·474 (3) | C(8)–C(11) | 1·480 (3) |
| C(3)–C(4) | 1·446 (3) | C(9)–C(10) | 1·445 (3) |
| C(4)–N(1*) | 1·398 (3) | C(10)–N(7*) | 1·393 (3) |
| C(4)–O(6) | 1·211 (3) | C(10)–O(12) | 1·214 (2) |
| C(3)–H(3) | 0·95 (2) | C(9)–H(9) | 0·92 (2) |
| C(5)–H(5*A*) | 0·97 (3) | C(11)–H(11*A*) | 0·96 (3) |
| C(5)–H(5*B*) | 0·97 (3) | C(11)–H(11*B*) | 0·99 (3) |
| C(5)–H(5*C*) | 1·03 (3) | C(11)–H(11*C*) | 0·95 (3) |
| C(2)–N(1)–N(1*) | 108·8 (2) | C(8)–N(7)–N(7*) | 108·8 (2) |
| C(2)–N(1)–C(4*) | 141·4 (2) | C(8)–N(7)–C(10*) | 141·6 (2) |
| N(1)–C(2)–C(3) | 107·8 (2) | N(7)–C(8)–C(9) | 108·0 (2) |
| N(1)–C(2)–C(5) | 120·4 (2) | N(7)–C(8)–C(11) | 120·6 (2) |
| C(3)–C(2)–C(5) | 131·7 (2) | C(9)–C(8)–C(11) | 131·4 (2) |
| C(2)–C(3)–C(4) | 110·4 (2) | C(8)–C(9)–C(10) | 110·1 (2) |
| C(3)–C(4)–N(1*) | 103·2 (2) | C(9)–C(10)–N(7*) | 103·5 (2) |
| C(3)–C(4)–O(6) | 133·0 (2) | C(9)–C(10)–O(12) | 133·0 (2) |
| O(6)–C(4)–N(1*) | 123·8 (2) | O(12)–C(10)–N(7*) | 123·5 (2) |
| C(4)–N(1*)–N(1) | 109·8 (2) | C(10)–N(7*)–N(7) | 109·6 (2) |

Table 7. *Bond distances* (Å) *and bond angles* (°) *in* $\mu$-$[C(CN)_2]$-*syn*-$(CH_2,CH_3)B$

| | | | |
|---|---|---|---|
| N(1)–N(5) | 1·394 (3) | | |
| N(1)–C(2) | 1·432 (4) | N(1)–C(8) | 1·438 (4) |
| C(2)–C(3) | 1·468 (4) | C(8)–C(7) | 1·467 (4) |
| C(2)–O(9) | 1·217 (4) | C(8)–O(10) | 1·207 (4) |
| C(3)–C(4) | 1·343 (4) | C(7)–C(6) | 1·337 (4) |
| C(3)–C(11) | 1·479 (5) | C(7)–C(12) | 1·489 (4) |
| C(4)–N(5) | 1·407 (4) | C(6)–N(5) | 1·405 (3) |
| C(4)–C(13) | 1·491 (4) | C(6)–C(14) | 1·491 (4) |
| C(13)–C(15) | 1·569 (4) | C(14)–C(15) | 1·565 (5) |
| C(15)–C(16) | 1·479 (4) | C(15)–C(17) | 1·489 (5) |
| C(16)–N(18) | 1·136 (5) | C(17)–N(19) | 1·133 (5) |
| N(5)–N(1)–C(2) | 107·4 (2) | N(1)–N(5)–C(4) | 108·2 (2) |
| N(5)–N(1)–C(8) | 107·7 (2) | N(1)–N(5)–C(6) | 108·3 (2) |
| C(2)–N(1)–C(8) | 127·9 (2) | C(4)–N(5)–C(6) | 121·4 (2) |
| N(1)–C(2)–C(3) | 106·0 (2) | N(1)–C(8)–C(7) | 105·3 (2) |
| N(1)–C(2)–O(9) | 123·1 (3) | N(1)–C(8)–O(10) | 124·1 (3) |
| C(3)–C(2)–O(9) | 130·8 (3) | C(7)–C(8)–O(10) | 130·6 (3) |
| C(2)–C(3)–C(4) | 107·5 (3) | C(8)–C(7)–C(6) | 108·2 (2) |
| C(2)–C(3)–C(11) | 122·9 (3) | C(8)–C(7)–C(12) | 122·2 (3) |
| C(4)–C(3)–C(11) | 129·6 (3) | C(6)–C(7)–C(12) | 129·6 (3) |
| C(3)–C(4)–N(5) | 110·4 (3) | C(7)–C(6)–N(5) | 110·3 (2) |
| C(3)–C(4)–C(13) | 135·6 (3) | C(7)–C(6)–C(14) | 136·2 (2) |
| N(5)–C(4)–C(13) | 114·0 (2) | N(5)–C(6)–C(14) | 113·5 (2) |
| C(4)–C(13)–C(15) | 109·2 (2) | C(6)–C(14)–C(15) | 108·0 (2) |
| C(13)–C(15)–C(14) | 111·0 (2) | C(16)–C(15)–C(17) | 107·6 (3) |
| C(13)–C(15)–C(16) | 109·7 (2) | C(14)–C(15)–C(16) | 108·5 (2) |
| C(13)–C(15)–C(17) | 108·1 (2) | C(14)–C(15)–C(17) | 111·8 (2) |
| C(15)–C(16)–N(18) | 177·4 (4) | C(15)–C(17)–N(19) | 176·4 (4) |

(I) and (II) to 1·406 Å in (III) while those involving the carbonyl C vary from 1·396 Å in (II) and 1·411 Å in (I) to 1·435 Å in (III). The C=C bond distances are essentially unaffected by the substitution of $CH_3$ for H at C(3) and C(7) (Goldberg *et al.*, 1982). The above correlations suggest that in the *planar* bimanes there is an apparent delocalization of the N nonbonding electrons into the ring system. According to the bond-length–bond-order curve proposed by Burke-Laing & Laing (1976) the observed interatomic distances in (I) and (II) correspond to approximate bond orders of N–N 1·2, N–C(=O) 1·15 and N–C(=C) 1·3. In agreement with previous observations in related heterocycles where the N atom is involved in three $\sigma$ bonds, the sum of the assumed bond orders around the N atoms exceeds the value of 3 (3·6–3·8). These bond orders would be slightly smaller if the effects of thermal motion on the bond lengths were included (see below). Evidently, a significantly lower degree of conjugation is present in the bridged molecule due to a more-$sp^3$-like hybridization around N. The differences in electron delocalization are also reflected in the bond orders related to C–C bonds. The

bond orders for the observed $C(sp^2)$–$C(sp^2)$ and $C(sp^2)$=$C(sp^2)$ distances are about 1·2 and 1·8 in (I), 1·2 and 2·0 in (II) and 1·05 and 2·0 in (III), which indicates that peripheral conjugation is more important in the planar *syn* derivative than in the other species.

The covalent bonding parameters of the 9,10-dioxabimane framework described above are considerably different from the corresponding quantities observed in other known structures containing five-membered pyrazolone rings: the most closely related structure is that of antipyrine (2,3-dimethyl-1-phenyl-5-pyrazolinone; Singh & Vijayan 1973, 1974). Apparently, the *syn* and *anti* bimanes are less conjugated than the pyrazolinone system. The observed geometry of the bicyclic bimanes mainly reflects delocalization of electron density within the central part of the molecule along the C–N–N–C=O chain. Structural forms which involve peripheral conjugation and charge separation (with formal negative charge on the O atoms and positive charge on the N) seem much less important than in a monocyclic pyrazolone. Correspondingly, the C=O bond lengths in the bimanes show only small variation and are characteristic of localized double bonds (1·21–1·22 Å); in the various antipyrine species (keto forms) these bonds are considerably longer (1·24 to 1·27 Å).

Introduction of a symmetric bridging ring at positions 4 and 6 of the bimane framework results in a bent and considerably strained tricyclic structure (III). The molecule is folded around the central N–N bond, preserving approximate $C_s$ symmetry. As a result, the C–N(5)–C angle is reduced to about 121° in comparison with 142° in compounds (I) and (II). This value is still larger, however, than that expected for an internal bond angle involving N in an unstrained six-membered ring (*ca* 112°). Moreover, bond angles around C(4) and C(6) show marked deviations from the observed values in unbridged bimanes. Thus, in (I) and (II) the exocyclic $CH_3$–C–N(5) and $CH_3$–C=C angles vary within 120–122° and 130–132° respectively; in the bridging molecule the corresponding values are about 114 and 136°. The endocyclic N(5)–C=C angles change in a complementary manner from about 108° in (I) and (II) to about 110° in (III). The effect of the steric strain on the molecular structure of (III) is also illustrated by the significantly stretched C(13)–C(15) and C(14)–C(15) bonds. The respective distances are 1·569 and 1·565 Å, as compared to the usually quoted reference value of 1·537 Å for a normal $C(sp^3)$–$C(sp^3)$ bond. Consequently, the chair conformation of the six-membered ring is flattened. The puckering angle on the side of the N is about 42, while that on the side of the $C(CN)_2$ group is about 51°. A very similar lengthening of a single $C(sp^3)$–$C(sp^3)$ bond (1·564 Å) was found in the zero-bridged bimane [*μ*-(−)-*syn*-($CH_2$,$CH_3$)B], which consists of three fused five-membered rings and is even more strained. The additional strain in the latter compound is apparently accommodated by an increased fold of the bimane framework, the observed dihedral angle being 129° (Kosower, Hermolin, Pazhenchevsky & Goldberg, 1981).

*Thermal motion*

An analysis of the vibrational tensors of the nonhydrogen atoms shows that the rigid-body approximation is not valid for the planar bimanes (I) and (II). The non-rigid-body behavior is due to excessive thermal vibrations of the central N atoms in a direction perpendicular to the molecular plane, which are significantly larger than the in-plane vibrations. The values listed below illustrate the vibration components along the three principal axes of inertia ($l$,$m$,$n$) of the bicyclic framework, the third component in each group being along the normal to the molecular plane: N(1) in (I) 0·025, 0·021 and 0·049 Å$^2$; N(5) in (I) 0·026, 0·022 and 0·051 Å$^2$; N(1) in (II) 0·034, 0·032 and 0·087 Å$^2$; N(7) in (II) 0·039, 0·024 and 0·107 Å$^2$. In both molecules the adjoining C atoms exhibit considerably more isotropic motion, their vibration components along $n$ ranging from 0·029 to 0·038 Å$^2$ in (I) and from 0·045 to 0·058 Å$^2$ in (II). In fact, the distinct anisotropy of the thermal parameters for the N may imply that the molecular structure is disordered in the solid, the observed results representing the average of (at least) two slightly bent forms of the bimane molecule. (A similar type of motion has been found in various crystals containing planar molecules of dibenzo-*p*-dioxin in which an O atom with a relatively small van der Waals radius is surrounded by 'larger' C atoms; Goldberg & Shmueli, 1973.) We estimate very roughly (by applying the 'riding-motion' concept) that the observed N–N and C–N bond distances in (I) and (II) could be artificially shortened by, at most, 0·009 Å due to the effect of such motion. However, in the absence of a reliable model, the exact influence of the internal vibrations on the molecular geometry remains unclear.

On the other hand, the 11-atom tricyclic framework of compound (III) is considerably less flexible in the solid. Both N atoms have a pyramidal configuration and are characterized by nearly isotropic thermal motion. Fitting the observed atomic thermal parameters to general rigid-body motions described by the **T**, **L** and **S** tensors results in a root-mean-square discrepancy of $\Delta U^{ij}$ of 0·025 Å$^2$ as compared to 0·017 Å$^2$, the mean e.s.d. of the observed $U^{ij}$. Since the librational vibrations appear to be small (maximum amplitude about 3·0°) in the rigid-body model, the possible corrections to the relevant bond lengths are 0·003 Å or less. When the peripheral O(9), O(10), C(11) and C(12) are included in the calculations, the discrepancy between the experimental and calculated parameters becomes slightly larger: $\langle(\Delta U^{ij})^2\rangle^{1/2} = 0{\cdot}034$ Å$^2$. As in many other compounds, thermal motion of the two

peripheral cyano groups is largely independent of that of the molecular framework.

*Deformation electron density map of syn-*$(CH_3,H)B$

The experimental deformation density distribution in the molecular plane is shown in Fig. 1(*b*). Due to the approximations involved (low-resolution data, relatively small data-to-parameters ratio) and unrigorous treatment of the H atoms in the model used, only the qualitative features of the map should be considered. The maximum density is found in the C–N bonds (0·45 e $Å^{-3}$), with a clear shift of valence electrons toward the more electronegative N atom. Polarization is more extreme in the N–C(=O) bonds than in the N–C(=C) bonds, probably as a result of the apparent repulsion between the bonding densities in the neighboring C=O and C–N bonds. The marked deficiency in $\sigma$ electron density near the carbonyl C is consistent with the fact that in most bimane moieties the adjacent N–C bonds are invariably longer (Goldberg *et al.*, 1982) and thermally less stable (Kosower & Pazhenchevsky, 1980) than the N–C bonds distant from the carbonyl. The disparity between the bond orders of N–C(=O) and N–C(=C) evident in our crystallographic data is also predicted by theoretical calculations; the total overlap populations for the two bonds are 0·841 and 0·762 respectively. High density is also found in the C–C ring bonds (peaks are at 0·30 and 0·35 e $Å^{-3}$), and maxima which could correspond to lone-pair electrons are clearly visible near the carbonyl O atoms. The peak of deformation density along the N–N bond is low (0·15 e $Å^{-3}$), in agreement with previous observations in the deformation densities of other compounds containing N–N bonds (Eisenstein, 1979).

It is of interest to compare these results with an *ab initio* SCF calculation at the 4-31G level, carried out with an extension of the *GAUSS* 70 program (Hehre, Lanthan, Ditchfield, Newton & Pople, 1976) as modified by Baudet & Port (1978). Due to limitations of computer memory, the peripheral methyl groups $CH_3(11)$ and $CH_3(12)$ were replaced in the structural model used by H atoms. One should keep in mind, however, that the theoretical maps which result from such calculations are not affected by thermal smearing, and that the basis set used is probably too small to give a reliable charge distribution. Nevertheless, many of the features present in the experimental map also appear clearly in the theoretical map (Fig. 5). For example, both maps show a deficient bonding density in the N–N bond and polarized densities in the N–C bonds (see above).

Fig. 5 shows that the *ab initio* deformation density maps for the *anti* isomer exhibit features similar to those observed for the *syn* isomer. We note in fact that the region above and below the N–N bond ($\pi$ bonding) is also dominated by negative or zero electron density.

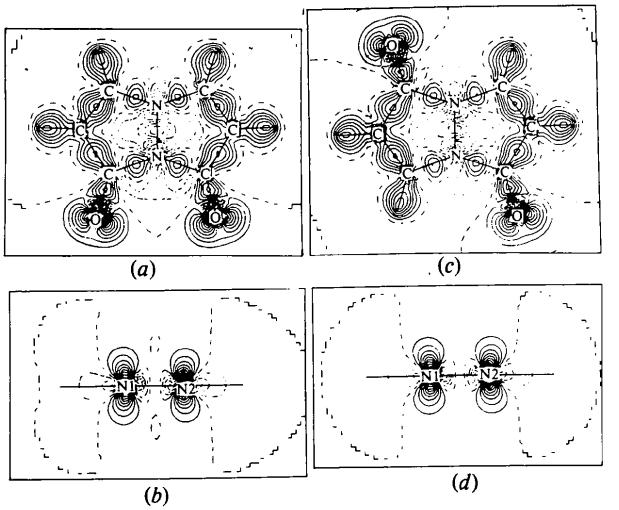


Fig. 5. Theoretical deformation electron density maps for (*a*), (*b*) *syn*-(H,H)B, and (*c*), (*d*) *anti*-(H,H)B. For (*a*) and (*c*) the view is on the molecular plane. Sections (*b*) and (*d*) are perpendicular to the respective molecular planes and contain the N–N bond. Contour intervals are 0·1 e $Å^{-3}$; solid lines indicate positive electron density, broad broken lines the zero level of electron density, and dashed lines regions of negative electron density.

This correlates with an observation that the calculated Mulliken $\pi$-overlap populations in the N–N region of both isomers have a non-bonding character. While the existence of the N–N bond is clearly established from chemical and crystallographic data, it appears that both the experimental and theoretical deformation maps fail to provide adequate evidence which would clarify the nature of this bond.

We have also carried out the calculations for the non-planar conformations of the *syn* and *anti* isomers, maintaining the experimental bond lengths and angles but with a dihedral angle of 143·4° about the N–N bond. Without allowing the bond lengths and bond angles to relax, the bent conformations are less favorable than the planar by 27·7 and 23·5 kJ for the *syn* and *anti* isomers respectively. This is probably a reasonable upper limit to the energy difference between conformers. The absolute values of the net atomic charges (Mulliken populations) on all atoms except the O and H atoms decrease upon bending the molecule in this manner.

*The intermolecular interactions*

The crystal structure of *syn*-$(CH_3,H)B$ shown in Fig. 6 consists of equivalent layers of molecules perpendicular to the *b* axis (at $y = \frac{1}{4}$ and $\frac{3}{4}$) which are related by a $2_1^b$ screw axis as well as by inversion. Within each layer there are two symmetry-equivalent molecules oriented nearly at right angles to one another. Such an arrangement minimizes electrostatic repulsions; it is apparently optimal for every molecule in the layer to be

involved in several relatively short CH···O interactions, such as: CH(7)···O(9) (at $\frac{1}{2}+x, \frac{1}{2}-y, \frac{1}{2}-z$) = 3·336 (4) [H···O = 2·45 (4)]; and $CH_3$(12)···O(10) (at $\frac{1}{2}+x, \frac{1}{2}-y, \frac{1}{2}-z$) = 3·242 (4) Å [H···O = 2·44 (3) Å]. Between the layers, molecules associate by forming infinite stacks of almost entirely overlapping species. At room temperature the perpendicular distances between the planes containing centrosymmetrically related bimanes is 3·325 Å, individual interatomic distances which involve O exceeding 3·45 Å. The interlayer arrangement in this structure resembles packing modes typical to $\pi$–$\pi^*$ molecular complexes (Prout & Kamenar, 1973). Since, however, neither in the crystal nor in solution is there any evidence for a charge-transfer absorption, we believe that the crystals of (I) are stabilized largely by dipolar interactions.

On cooling the crystal from 300 K to the temperature at which the phase transition occurs (~183 K), the principal thermal contraction is along the stacking axis *b* (Table 1), and the distance between successive molecular planes in this direction is reduced to 3·273 Å. This behavior suggested that (I) might exhibit a propensity for undergoing a phase transition or a solid-state dimerization along **b** (*via* the formation of N–N bonds between the adjacent overlapping bimanes), when exposed to high pressures. To test this hypothesis, crystals of (I) were subjected to pressures up to 4·5 GPa at room temperature in a diamond-anvil cell which could be monitored both visually and *via* X-ray diffraction (Piermarini, Mighell, Weir & Block, 1969; Block, Weir & Piermarini, 1970). However, neither a reaction nor any evidence of a phase change was observed under these conditions.

Fig. 7 illustrates the packing of the *anti*-($CH_3$,H)B structure in its unit cell. The two independent molecules centered at 0,0,0 (*A*) and 0,0,$\frac{1}{2}$ (*B*) are almost exactly parallel to each other, the molecular plane of *A* being rotated by about 57° with respect to that of *B*.

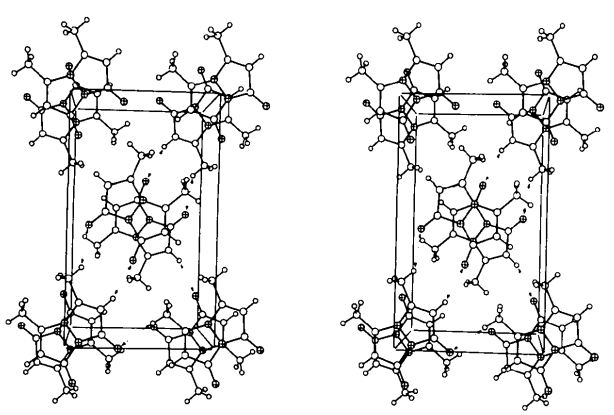

Fig. 6. Stereoscopic view of the crystal structure of *syn*-($CH_3$,H)B along a direction slightly tilted to **b**. Several intermolecular C–H···O interactions are shown by dashed lines.

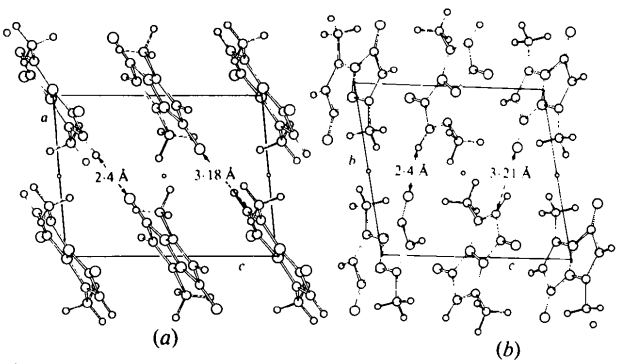


Fig. 7. Two parallel projections of the crystal structure of *anti*-($CH_3$,H)B (*a*) on the *ac* plane and (*b*) on the *bc* plane, showing intermolecular C–H···O contacts (see text for a detailed description).

The crystal structure can be described as composed of sheets of molecules which extend parallel to the $(1\bar{1}2)$ plane, and these are very similar to those found in the structure of (I). Within the layers every molecule of type *A* (or equivalently *B*) is surrounded by four molecules of type *B* (or *A*) and involved in four CH···O lateral interactions. The C atoms which donate the H are C(3) and C(9), and the acceptors are the carbonyl O atoms: CH(3)···O(12) (at $x, y-1, z$) = 3·209 (3) [H···O = 2·40 (4)] (Fig. 7*b*), and CH(9)···O(6) (at $x-1, y, z$) = 3·182 (3) Å [H···O = 2·37 (4) Å] (Fig. 7*a*). While the intralayer arrangement is associated with the extensive two-dimensional arrays of C–H···O attractions, the interlayer structure arises from stacking and (local) dipolar interactions. Thus, the crystal contains infinite stacks of overlapping parallel molecules of *A* and *B* (in an alternating order) which extend along the *c* axis. Each molecule is effectively in close packing with two neighbors located 3·38 ± 0·01 Å below and above its mean plane. There are no interatomic contacts shorter than the expected van der Waals distances within these stacks. Relatively short non-bonding distances are between methyl groups of adjacent molecules displaced along **a** + **b** which are related by inversion: $CH_3(11)\cdots CH_3(11)$ (at $1-x, 1-y, -z$) = 3·660 (4), $CH_3(5)\cdots CH_3(5)$ (at $1-x, 1-y, 1-z$) = 3·719 (4) Å.

There exists an interesting similarity between the crystal structures of (I) and (II) and that of pyridazino-[1,2-*a*]pyridazine-1,4,5,8-tetrone (Laing, Sommerville & Piacenza, 1977), in spite of the fact that they are characterized by different space symmetry (the respective space groups are *Pnma*, $P\bar{1}$ and $P2_1/c$). All three structures consist of molecular layers of planar or nearly planar bicylic species, and are stabilized by almost identical arrays of C–H···O=C and stacking interactions.

Fig. 8 shows the packing diagram of $\mu$-[C(CN)$_2$]-*syn*-($CH_2$,$CH_3$)B. The bridged molecules are efficiently

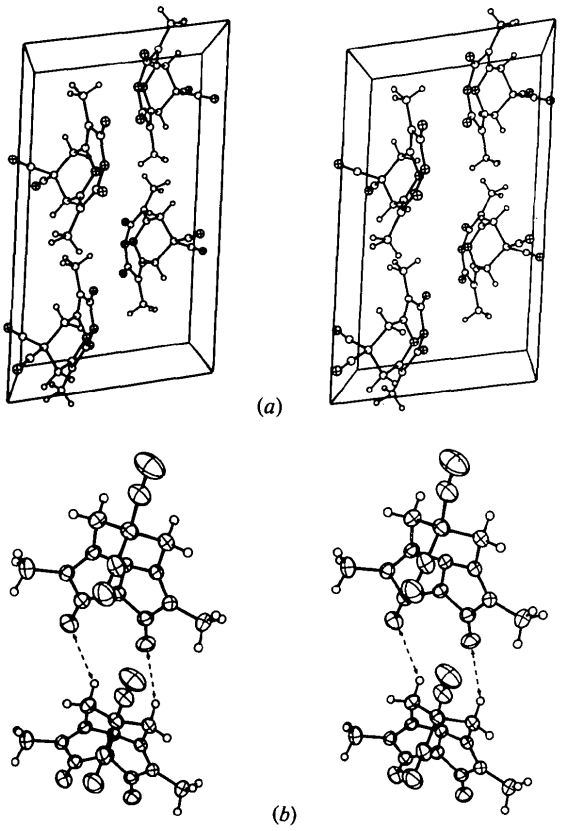

Fig. 8. Stereoscopic illustrations of the crystal structure of $\mu$-[$C(CN)_2$]-*syn*-($CH_2$,$CH_3$)B. (*a*) Contents of the unit cell viewed along a direction slightly tilted to **b**. (*b*) The C—H···O-type association between adjacent molecules displaced by **b**.

stacked along the shortest dimension of the cell, the convex part of one species being in close contact with the concave side of its neighbor along the stack. A feature of further significance in this structure is the C—H···O-type association between adjacent bimane molecules displaced by **b**. Each molecule participates in four interactions of this kind *via* the C(13) and C(14) methylene groups as H donors and the carbonyl O atoms as H acceptors. Relevant non-bonding distances are: $CH_2(13)\cdots O(9)$ (at $x$, $1+y$, $z$) = 3·262 (4) (H···O = 2·43) and $CH_2(14)\cdots O(10)$ (at $x$, $1+y$, $z$) = 3·353 (4) Å (H···O = 2·63 Å). The latter seems less efficient due to steric hindrance introduced by a close packing of the molecules about the screw axes, which is reflected in relatively short distances between O(10) (at $x,y,z$) and C(6), C(7) and C(12) (at $1-x$, $\frac{1}{2}+y$, $\frac{1}{2}-z$) of 3·201 (4), 3·027 (4) and 3·309 (5) Å respectively. All other contacts are equal to or longer than the normal van der Waals contacts. The polar cyano substituents of different species are arranged in a favorable antiparallel manner across crystallographic centers of inversion.

Extensive arrays of specific C—H···O interactions similar to those observed in the crystal structures of (I), (II) and (III) exist also in the structures of $\mu$-($SO_2$)-*syn*-($CH_2$,$CH_3$)B, $\mu$-(S)-*syn*-($CH_2$,$CH_3$)B (Goldberg, 1980) and *syn*-(H,Cl)B (Goldberg & Kosower, 1982). Summarizing the geometric parameters of these interactions in bimane crystals we find that the C···O and H···O distances vary between 3·20–3·35 and 2·2–2·6 Å (values based on the experimental but under-determined C—H bond lengths) respectively. The observed C—H···O angles range from 130 to 175°. The methylene groups in (III) are certainly activated because they are bound directly to an electron-withdrawing dicyanomethylene substituent. Moreover, the significance of C—H···O interactions involving protons attached to C at positions 3 and 7 of the bimane framework is reflected in: (*a*) the consistency found in the packing arrangements of compounds (I), (II) and pyridazino[1,2-*a*]pyridazine-1,4,5,8-tetrone (see above); and (*b*) a more efficient crystal packing of (II) ($D_c$ = 1·369 Mg $m^{-3}$) than that of its heavier analog, *anti*-($CH_3$,$CH_3$)B (space group $P2_1/c$, $D_c$ = 1·305 Mg $m^{-3}$; Bernstein, Goldstein & Goldberg, 1980). In fact, theoretical MO calculations indicate that the net atomic charges are slightly negative at positions 3 and 7 and considerably more positive at other C atoms of the bicyclic framework. Thus, the participation of H atoms at positions 3 and 7 in C—H···O 'bonds' emphasizes the significance of these interactions.

Experimental evidence for C—H···O bonding with methyl, methylene and $\geqslant$C—H groups as H donors has repeatedly been described in recent literature (*e.g.*, Bernstein, Cohen & Leiserowitz, 1974; Goldberg, 1975; Schomberg, 1980; Batail, LaPlaca, Mayerle & Torrance, 1981). We tentatively conclude, therefore, that such bonding also provides a structure-determining contribution in the crystals of the bimane species referred to above.

The cooperation of many people made this work possible. Barak Pazhenchevsky provided crystals. Professor K. N. Trueblood of UCLA made his diffractometer available for low-temperature measurements of (I) and also provided hospitality for one of us (IG). Computer time and invaluable assistance at the Weizmann Institute were provided by Professor D. Rabinovich, Dr Peter Stern and Ms Pnina Dauber. Ehud Goldstein of Ben-Gurion University also aided in some of the computational work. Drs Stanley Block and Gaspar Piermarini carried out the high-pressure studies on (I).

## References

BATAIL, P., LAPLACA, S. J., MAYERLE, J. J. & TORRANCE, J. B. (1981). *J. Am. Chem. Soc.* **103**, 951–953.

BAUDET, J. & PORT, G. N. H. (1978). Private communication to A. T. HAGLER.

BERNSTEIN, J., COHEN, M. D. & LEISEROWITZ, L. (1974). *The Chemistry of Quinonoid Compounds*, edited by S. PATAI, pp. 37–110. New York: John Wiley.
BERNSTEIN, J., GOLDSTEIN, E. & GOLDBERG, I. (1980). *Cryst. Struct. Commun.* **9**, 295–299, 301–305.
BLOCK, S., WEIR, C. E. & PIERMARINI, G. J. (1970). *Science*, **169**, 586–587.
BRAUN, P. B., HORNSTRA, J. & LEENHOUTS, J. I. (1969). *Philips Res. Rep.* **24**, 85–118.
BURKE-LAING, M. & LAING, M. (1976). *Acta Cryst.* B**32**, 3216–3224.
DUNITZ, J. D. & SEILER, P. (1973). *Acta Cryst.* B**29**, 589–595.
EISENSTEIN, M. (1979). *Acta Cryst.* B**35**, 2614–2625.
GOLDBERG, I. (1975). *Acta Cryst.* B**31**, 754–762, 2592–2600.
GOLDBERG, I. (1980). *Cryst. Struct. Commun.* **9**, 329–333.
GOLDBERG, I., BERNSTEIN, J. KOSOWER, E. M., GOLDSTEIN, E. & PAZHENCHEVSKY, B. (1982). Unpublished results.
GOLDBERG, I. & KOSOWER, E. M. (1982). *J. Phys. Chem.* **86**, 332–335.
GOLDBERG, I. & SHMUELI, U. (1973). *Acta Cryst.* B**29**, 432–440.
HEHRE, W. J., LANTHAN, W. A., DITCHFIELD, R., NEWTON, N. W. & POPLE, J. A. (1976). *Quantum Chemistry Program Exchange*. Indiana Univ., Bloomington, Indiana. Program No. 236.
HIRSHFELD, F. L. (1977). *Isr. J. Chem.* **16**, 226–229.
HUPPERT, D., DODIUK, H., KANETY, H. & KOSOWER, E. M. (1979). *Chem. Phys. Lett.* **65**, 164–168.
*International Tables for X-ray Crystallography* (1974). Vol. IV, pp. 71–98. Birmingham: Kynoch Press.
KOSOWER, E. M., HERMOLIN, J., PAZHENCHEVSKY, B. & GOLDBERG, I. (1981). Unpublished results.
KOSOWER, E. M. & PAZHENCHEVSKY, B. (1980). *J. Am. Chem. Soc.* **102**, 4983–4993.
KOSOWER, E. M., PAZHENCHEVSKY, B., DODIUK, H., KANETY, H. & FAUST, D. (1981). *J. Org. Chem.* **46**, 1666–1673.
KOSOWER, N. S., KOSOWER, E. M., ZIPSER, Y., FALTIN, Z. & SHOMRAT, R. (1981). *Biochim. Biophys. Acta*, **640**, 748–759.
KOSOWER, N. S., NEWTON, G. L., KOSOWER, E. M. & RANNEY, H. M. (1980). *Biochim. Biophys. Acta*, **622**, 201–209.
LAING, M., SOMMERVILLE, P. & PIACENZA, L. P. L. (1977). *Acta Cryst.* B**33**, 2464–2471.
MAIN, P., WOOLFSON, M. M., LESSINGER, L., GERMAIN, G. & DECLERCQ, J. P. (1974). *MULTAN* 74. *A System of Computer Programs for the Automatic Solution of Crystal Structures from X-ray Diffraction Data*. Univs. of York, England, and Louvain, Belgium.
PIERMARINI, G. J., MIGHELL, A. D., WEIR, C. E. & BLOCK, S. (1969). *Science*, **165**, 1250–1255.
PROUT, C. K. & KAMENAR, B. (1973). *Molecular Complexes*. Vol. I, ch. 4, edited by R. FOSTER. London: Elek Science.
SCHOMBERG, D. (1980). *J. Am. Chem. Soc.* **102**, 1055–1058.
SINGH, T. P. & VIJAYAN, M. (1973). *Acta Cryst.* B**29**, 714–720.
SINGH, T. P. & VIJAYAN, M. (1974). *Acta Cryst.* B**30**, 557–562.
STEWART, R. F., DAVIDSON, E. R. & SIMPSON, W. T. (1965). *J. Chem. Phys.* **42**, 3175–3187.

*Acta Cryst.* (1982). B**38**, 2000–2004

# Structures of Inorganic Rings as Antitumor Agents. III.* Structures of the Monoclinic and Orthorhombic Forms of 2,2,4,4,6,6-Hexa(1-aziridinyl)cyclotri(phosphazene), $N_3P_3az_6$

BY T. STANLEY CAMERON†

*Department of Chemistry, Dalhousie University, Halifax, Nova Scotia, Canada B3H 4J3*

AND JEAN-FRANÇOIS LABARRE AND MARCEL GRAFFEUIL

*Laboratoire Structure et Vie, Université Paul Sabatier, 118 route de Narbonne, 31400 Toulouse, France*

(*Received* 16 *October* 1981; *accepted* 1 *February* 1982)

## Abstract

$P_3N_3[N(CH_2)_2]_6$, $C_{12}H_{24}N_9P_3$, $M_r = 387{\cdot}3$; form (I): orthorhombic, $a = 7{\cdot}981\ (2)$, $b = 13{\cdot}641\ (3)$, $c = 16{\cdot}589\ (3)$ Å, $Z = 4$, $D_c = 1{\cdot}424$ g cm$^{-3}$, $\mu = 2{\cdot}93$ cm$^{-1}$, space group $P2_12_12_1$, 1030 observed reflections, $R = 0{\cdot}027$; form (II): monoclinic, $a = 9{\cdot}626\ (2)$, $b = 8{\cdot}099\ (3)$, $c = 23{\cdot}67\ (1)$ Å, $\beta = 101{\cdot}39\ (3)°$, $Z = 4$, $D_c = 1{\cdot}420$ g cm$^{-3}$, $\mu = 2{\cdot}92$ cm$^{-1}$, $P2_1/c$, 998 observed reflections, $R = 0{\cdot}053$. Monochromatic Mo $K\alpha_1$ radiation ($\lambda = 0{\cdot}70926$ Å) was used. The structures were solved by the direct method. The molecule in each of the two forms has a very similar conformation with the geminal aziridinyl groups adopting the *trans* arrangement.

* Part II: Cameron, Labarre & Graffeuil (1982).
† To whom correspondence should be addressed.

0567-7408/82/072000-05$01.00 